Adv Syst Sci Appl 2021; **01**; 22-45
Published online at https://ijassa.ipu.ru.

Design and Comparison of Plasma H_∞ Loop Shaping and RGA-H_∞ Double Decoupling Multivariable Cascade Magnetic Control Systems for a Spherical Tokamak

Yuri Mitrishkin[1,2*], Evgeniia Pavlova[2], Mikhail Patrov[3]

1) Faculty of Physics, Lomonosov Moscow State University, Moscow, Russia

E-mail: y_mitrishkin@hotmail.com

2) V. A. Trapeznikov Institute of Control Sciences of the Russian Academy of Sciences, Moscow, Russia

E-mail: pavlova@physics.msu.ru

3) Ioffe Institute of the Russian Academy of Sciences, Saint Petersburg, Russia

E-mail: michael.patrov@mail.ioffe.ru

Abstract: The article aims to present an approach to design and compare cascade H_∞ loop shaping and essentially new cascade RGA-H_∞ double decoupling magnetic control systems for a multivariable dynamical plant, specifically plasma in a vertically elongated tokamak. Identification of the present control closed-loops containing a plasma linear model of a relatively high order for the spherical Globus-M tokamak (Ioffe Institute, St Petersburg, Russia) to derive a low order linear model (without the application of reduction algorithms) as a plant under control is undertaken. A robust H_∞ loop shaping method was applied to the identified model to design a plasma position, current, and shape (6 gaps between the first wall and plasma separatrix) multivariable controller. A structural analysis was done to get the most effective structure of the square plant with the 3rd gap eliminated in the feedback and a separate loop for the plasma current control. The methodology of the relative gain array (RGA) was applied to this structure to choose the proper correspondences between inputs and outputs (pairing), which brought the plant model closer to a decoupling plant (first decoupling in the open plant model). Further, the H_∞ adjustment of the control system with the pairing plant and an additional feedback decoupling matrix (second decoupling of the plant model in the feedback) and PI controllers in the feedback gave increased control system accuracy while tracking references. Comparison of the two control systems designed has shown that double decoupling gives higher performance accuracy and a less robust stability margin, while the robust loop shaping method allows the stability margin to be increased but gave less accurate control of the gaps.

Keywords: tokamak, plasma control, identification, structural analysis, decoupling

1. INTRODUCTION

1.1. State-of-the-art

A number of plasma magnetic control systems were designed and applied in simulations and experiments on a set of operating tokamaks with vertically elongated plasmas (JET, ASDEX Upgrade, TCV, DIII-D, EAST, KSTAR, JT-60U, NSTX, MAST, and others) and in simulations for ITER (International Thermonuclear Experimental Reactor). The survey [21] showed that there is a set of existing approaches which are used for the development of plasma magnetic control systems, for example, robust H_∞ control [1, 28], MPC [5], adaptive

* Corresponding author: y_mitrishkin@hotmail.com

MPC [20], cascade control [10, 27, 35], state control by LMI [32], etc. and allow the desired objectives to be achieved.

1.2. Motivation

However, multivariable plasma control systems are very far from a satisfactory level concerning their performance (accuracy and speed of response) and robustness (required stability margins) in confining the plasma with thermonuclear reactions inside vacuum vessels of future tokamak-reactors and tokamak power plants with high reliability and survivability. Therefore, at present they require further detailed development, like any other technology for fusion, e.g. materials for the first wall and diverter plates.

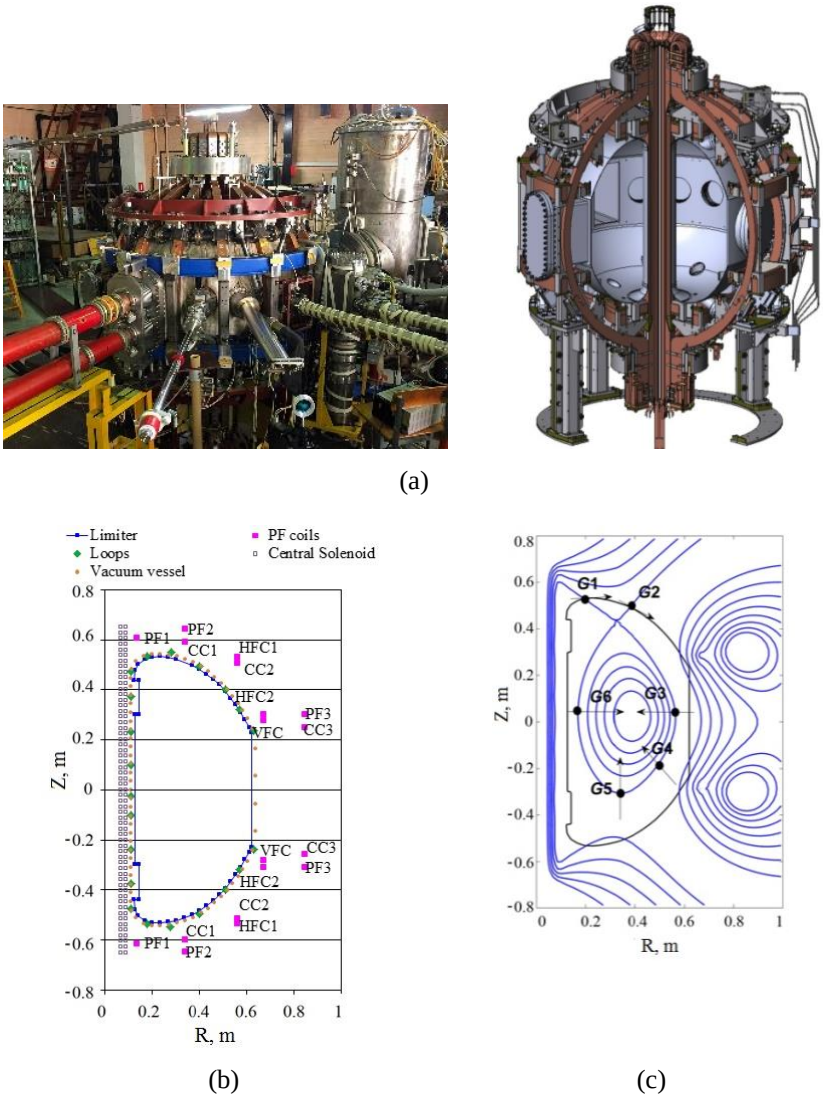

Fig. 1. (a) Spherical Globus-M tokamak, (b) vertical cross- section of Globus-M tokamak where PF, CC, HFC, and VFC are poloidal, correction, horizon and vertical field coils, and (c) plasma magnetic configuration with points G1-G6 and directions for gaps control [11]

Globus-M2 [18] belongs to a new generation of spherical tokamaks and it was launched in 2018. It is the same size as Globus-M (Fig. 1) [7, 8, 9] (plasma major radius $R \approx 36$ cm, minor radius $a \approx 24$ cm, elongation ≈ 2), but a new electromagnetic system allows a higher toroidal magnetic field and plasma current to be achieved. In 2018 the first plasma was obtained; discharges with $B_T = 0.5$ T, $I_p = 0.2$ MA, which correspond to the parameters of the last Globus-M experimental campaign [2], were demonstrated [17]. The first experimental campaign with the toroidal magnetic field of 0.7 T and the plasma current up to 300 kA was

carried out in 2019. The increase in toroidal magnetic field and plasma current resulted in an overall improvement of the discharge parameters. Significant plasma temperature growth and neutron rate increase was obtained. Record stored energy, which is approximately one and a half times higher than in the Globus-M experiments, was reached. The toroidal lower hybrid wave launch provided noticeable current drive. Preparation for the next experimental campaigns with a higher toroidal magnetic field and plasma current is underway. In future campaigns Globus-M2 will operate at designed parameters up to B_T = 1 T, Ip = 0.5 MA. The experiments will be centred around the reactor-relevant issues: current drive, energy and fast ion confinement, non-inductive plasma current start-up, diverter and SOL plasma studies.

The poloidal system of the Globus-M2 tokamak is unique because it is combined: some of the PF-coils are located inside the toroidal field coil and some are located outside that coil. In most tokamaks, the PF-coils are located completely inside or outside the toroidal field coil [24] or inside the vacuum vessel [21]. The Globus-M2 tokamak operates with a diverter plasma configuration similar to ITER (France). The power density of the plasma heating in Globus-M2 is several times higher than in the larger existing foreign tokamaks: JET (Great Britain), DIII-D (USA), ASDEX Upgrade (Germany), TCV (Switzerland). Tests of the key elements of the diagnostic systems of ITER are conducted on the Globus-M2 tokamak to support ITER. Because of that, we intend to design and simulate plasma control systems for the tokamak Globus-M, which is one of the advanced spherical tokamaks.

1.3. Application of standard control theory methods

A set of standard control theory methods was applied to the existing multivariable feedback multi-loop and cascade control system of Globus-M to design and find the best control system structures for plasma current and shape control on plasma linear models from the point of view of performance and robustness (H_∞ optimisation theory, H_∞ decoupling techniques, multilevel control theory, μ-analysis, identification by means of the subspace method, relative gain array approach, singular value frequency responses). The applied control methods of system design and analysis are known, but the results of their application to a plasma in a tokamak are new.

The design and simulation of hierarchical plasma control systems for Globus-M are done in line with the *original methodology* developed in [22].

1.4. Results and their novelty obtained for a plasma in a tokamak

Identification subspace methodology (not standard reduction methods of linear models) [14] was applied to the linear plasma position and PF-currents control systems containing plasma linear models to reduce their high order to an essential lower order so as to design plasma current and shape multivariable control systems. This approach imitated the application of the identification procedure to real control systems used in experiments to get identified linear models for the design of robust controllers which should enable the efficiency of closed-loop control systems.

The *H_∞ robust loop shaping method* [16] was applied to the identified (reduced) plasma model to design a plasma shape (6 gaps between the first wall and plasma separatrix and 5 PF-currents) multivariable controller in the presence of tuned PID-controllers inside the plasma position and PF-currents control circuits. At the same time, the normalised coprime factorised plant transfer function with perturbations in factors is shaped by input and output weighting functions, then a robust feedback controller is found to maximise the robust stability margin. The final controller contains the robust controller and weighting functions used.

Four structures were analysed by *singular value frequency responses* [34] with the 3rd or 4th gap eliminated in the feedback and a separate loop for the plasma current control to get the most effective structure of the square plant without the 3rd gap.

The *square* plant model obtained was used to design a *decentralised multivariable PI-controller* by means of a new *double decoupling*: (i) pairing of inputs/outputs in line with the RGA matrix [34] and (ii) fixed structure H_∞-tuning in the presence of an additional decoupling matrix in the feedback [4]. The two plasma shape control systems designed by the H_∞-robust loop shaping approach and by the double decoupling approach were compared using performance and robustness criteria. The first system showed a higher robust stability margin and the second one demonstrated better accuracy while tracking the plasma separatrix.

1.5. Paper structure

The paper is organised as follows. In Section 2, the control problem is formulated using the linear dynamic model of the plasma. In Section 3 the identification procedure and in Section 4 cascade H_∞ loop shaping controller design are represented. Section 5 is devoted to input–output analysis of multi-loop system structures. Section 6 discusses loop pairing and introduces the H_∞ double decoupling plasma shape control system design and simulation for square plant. The comparison of the two systems is presented in Section 7. In conclusion the results obtained are summarised.

2. CONTROL PROBLEM STATEMENT

2.1. Parameters of the Globus-M tokamak

The plasma in the Globus-M tokamak (Fig. 1, (a)) is the plant of the current investigation [7] with the following parameters: the maximum plasma current $I_{p\,\max} = 0.35$ MA, the maximum toroidal magnetic field $B_{t\,\max} = 0.6$ T, the major radius $R_0 = 0.36$ m, the minor radius $a_p = 0.24$ m, the aspect ratio $A = R_0/a_p = 1.5$, and the maximum vertical elongation $k_{\max} = 2.2$.

2.2. Plasma magnetic control system of the Globus-M/M2 tokamak

The plasma control multivariable and cascade system which is used by the Globus-M tokamak to control the plasma vertical (Z) and horizontal (R) positions (with the diagnostics system to assess the vertical and horizontal position of the plasma), the current in the central solenoid (CS), and the currents in the poloidal field (PF) coils are demonstrated in Fig. 2.

2.3. Linear model of the Globus-M/M2 plasma

The linear state space model for the plasma in the tokamak [22, 23], in line with the block diagram of Fig. 2, can be written in the general form with concrete matrices:

$$\dot{x} = Ax + Bu,\ y = Cx + Du$$

where $A_{75\times75}$, $B_{75\times8}$, $C_{39\times75}$, $D_{39\times8}$ are matrices of the model. The outputs of the plant model are as follows:

$$y = \left[\delta Z\ \ \delta R\ \ \delta I_p\ \ \delta I_{HFC}\ \ \delta I_{VFC}\ \ \delta I_{CS}\ \ \delta I_{PF}\ \ \delta I_{CC}\ \ \delta g^T\right]^T$$

where δZ, δR are plasma vertical and horizontal displacements, δI_p is the variation of the plasma current, δg are variations of the gaps between the separatrix and the first wall (Fig. 1, (c)), δI_{HFC}, δI_{VFC}, δI_{CS}, δI_{PF}, and δI_{CC} are variations of currents in corresponding poloidal field coils (Fig. 1, (b)). The inputs of the plant model are as follows:

$$u = \left[\delta U_{HFC}\ \ \delta U_{VFC}\ \ \delta U_{CS}\ \ \delta U_{PF}\ \ \delta U_{CC}\right]^T$$

where δU_{HFC}, δU_{VFC}, δU_{CS}, δU_{PF}, and δU_{CC} are variations of voltages on the HFC, VFC, CS, PF, and CC coils, respectively. The state vector x includes variations of currents in active coils and passive structures (the vacuum vessel) (Fig. 1, (b)).

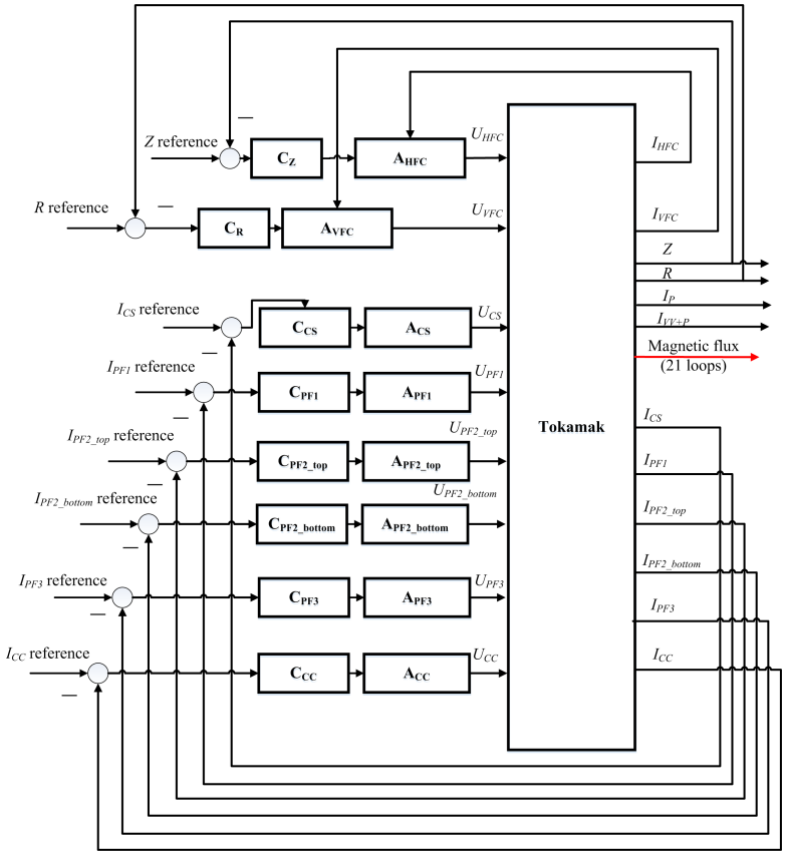

Fig. 2. Block diagram of the plasma control system operating in the Globus-M/M2: C_Z, C_R, C_{CS}, C_{PF1}, C_{PF2_top}, C_{PF2_bottom}, C_{PF3}, and C_{CC} are analogue controllers, A_{HFC}, A_{VFC}, A_{CS}, A_{PF1}, A_{PF2_top}, A_{PF2_bottom}, A_{PF3}, and A_{CC} are actuators.

2.4. Aims of the feedback control system design

The main control goal is to develop a plasma position (vertical and horizontal), current and shape control system for the Globus-M tokamak. The principal challenge is to build the feedback plasma shape control system. Currently the plasma shape control on Globus-M is carried out by means of program PF-currents, but there is no actual feedback shape control system on the Globus-M tokamak (Fig. 2). The problem of choosing a particular structure for the control system and the problem of tuning the multivariable controllers in this system are solved in this article. The structure of the control system has a significant effect on the characteristics of the closed-loop system, such as its stability and performance (speed of response and accuracy) as well as its robustness, so it is important to consider the structure in detail.

2.5. Controllers to be designed

Two types of plasma shape controllers: an H_∞ controller obtained by means of the loop shaping design procedure [15, 16] and a double decoupling PI-controller obtained by means of the RGA [34] and structured H_∞ synthesis [4], are to be designed and compared in terms of performance and robustness. These two approaches to the synthesis of control systems allow minimizing a single performance criterion, but the distinctive feature of the second approach is the decoupling of the plant.

- H_∞ robust control based on open-loop shaping

The H_∞ loop shaping design procedure consists of two stages: loop shaping and robust stabilisation [15, 16]. During the first stage the singular values of the plant model G_0 are shaped by shaping the inputs and outputs of the plant using the pre- and post-compensators

(W_1 and W_2) in order that the shaped plant model $G = W_2G_0W_1$ has large minimum singular values at low frequencies and small maximum singular values at high frequencies. At the second stage the robust stabilisation problem is solved for the shaped plant in relation to an H_∞-controller K_∞ in the feedback. In doing so, a robust stability margin of the closed-loop system is derived as follows:

$$\varepsilon_{\max} = 1/\inf_{K_\infty} \left\| \begin{bmatrix} I \\ K_\infty \end{bmatrix} \left(I + GK_\infty\right)^{-1} M^{-1} \right\|_\infty ,$$

where $M^{-1}N$ is a normalised left coprime factorisation of the shaped plant model. The final feedback controller includes the pre- and post-compensators W_1 and W_2: $K = W_1 K_\infty W_2$.

- Double decoupling with PI-control

First decoupling in the open-loop plant model is done using the methodology of the relative gain array (RGA) and, as a consequence, the proper pairing between model inputs and outputs, which decreases the interactions between control channels [34]. The loop pairing problem defines the control system structure, i.e., which of the available plant inputs are to be used to control each of the plant outputs. Variable pairing is used to establish the one-to-one mapping relationship between manipulated and controlled variables, and then decentralised feedback control loops can be tuned and implemented. The loop pairing decision should be done independently, such that any controller type could be designed after loop pairing.

The second decoupling of the plant model in the feedback is done using H_∞ fixed-structure adjustment of the control system with the pairing plant model, an additional feedback decoupling matrix, and PI-controllers in the feedback [4].

- Comparison of the approaches and plant model

In the case of the H_∞ robust control system design by the loop shaping approach of McFarlane and Glover [15, 16], the open-loop plant model is shaped by pre- and post-weighting functions to get proper frequency singular values characteristics, and then the shaped plant model is used in the feedback to design the H_∞-controller by maximising the robust stability margin of the closed-loop system as the single optimisation criterion.

In the case of the fixed-structure H_∞ control approach of Gahinet and Apkarian [4], the structure of the closed-loop control system is given by a designer and then the mixed sensitivity problem is solved by minimisation of the H_∞-norm of the stacked transfer matrix of sensitivity, and complementary sensitivity with weighting functions as another optimisation criterion.

In both cases of plasma shape control in the Globus-M tokamak, the plant model consists of a number of control closed loops of CS&PF-currents, where the references are the inputs (Fig. 2) and a plasma equilibrium reconstruction algorithm (not shown in Fig. 2) [11] to provide the model outputs, namely gaps between the separatrix and the first wall. The other output values are measured by tokamak diagnostics, specifically the CS&PF-currents, plasma current, horizontal and vertical plasma displacements [22].

2.6. Goals of plasma control

The outputs δR, δZ, δI_p, and δg are to be controlled by means of feedback of the plasma control system. The errors of these values to be controlled are the following:

$e_R = r_R - R$, $e_Z = r_Z - Z$, $e_{I_p} = r_{I_p} - I_P$, $e_{g_j} = r_{g_j} - g_j$, $\quad j = 1,...,6$.

The control problem can be stated as the need to achieve specified accuracy of the control in the finite time intervals:

$$\left|e_R(t)\right| < \varepsilon_R,\ t \in [t_1,\quad T],\ \left|e_Z(t)\right| < \varepsilon_Z,\ t \in [t_2,\quad T],$$

$$\left|e_{I_p}(t)\right| < \varepsilon_{I_p},\ t \in [t_3,\quad T],\ \left|e_{g_j}(t)\right| < \varepsilon_{g_j},\ t \in [t_4,\quad T],$$

where $t_1,...,t_4$ are time moments when the proper output values enter into desired bounds determined by positive constants ε_R, ε_R, ε_{I_p} and ε_{g_j} after transient responses which are caused by the tracking procedure. These time moments $t_1,...,t_4$ are different because of the different plant dynamics along the different channels under control. The time moment T is the moment of finishing the control procedures because plasma discharges in a tokamak are restricted in time.

It is important to meet stability requirements in the control system design. Stability margins may be specified and obtained by means of the small gain theorem when the result of multiplication of the H_∞-norms of the transfer functions of the uncertainty Δ and the known part of the system Q is less than 1: $\|\Delta\|_\infty \|Q\|_\infty < 1$. In that case, the μ-analysis gives useful results [28, 36].

3. IDENTIFICATION OF PLASMA POSITION, CURRENT, AND SHAPE CLOSED-LOOPS

3.1. Obtaining high order models to be identified

To develop the plasma control system, it is often useful to deal with low-dimensional models to design low- order controllers so that these controllers are able to determine the system dynamics during the quasi-stationary phase of plasma discharge with sufficient accuracy. To obtain the simplified, low-order model, one can use a model reduction technique [34] or an identification method [13, 14]. The linear model of the plant under control with a reduced order was produced as a result of the identification of the full (the 75th order) model [11, 31] obtained on the basis of the experimental data of the tokamak Globus-M [23]. The outputs of the aforementioned 75-dimensional model were used as the outputs of the real-time Globus-M tokamak. The order of the model comes from the plasma in a tokamak and actuators which are connected in series with the tokamak (Fig. 2).

Before the beginning of the simulation, the unstable linear model was vertically stabilised by an automatically adjusted PID-controller included in the feedback at a predetermined point of the scenario. The PID-controller was tuned using the PID Tuner app in MATLAB. This app allows one to achieve a balance between performance and robustness while tuning the gains of a controller for a SISO plant. Then the testing reference signals were fed to the input of the closed loop system (Fig. 3(1)).

The testing signals were fed to the four control loops as a novel series one by one (Fig. 3):

(1) vertical and

(2) horizontal position control loops,

(3) plasma current control loop,

(4) gaps between the separatrix and the first wall control loop.

All these PID- controllers were also synthesized using the PID Tuner app in MATLAB.

Since, as noted above, the numerical experiment was carried out at one point of the scenario, the first half of the plasma discharge was used for identification and the second half was used for verification of the obtained models. There are two types of actuators in the closed loop system, namely, thyristor current inverters [12] and multiphase thyristor rectifiers [29].

The current inverters are complex nonlinear impulse converters based on thyristor bridges working in self-oscillatory mode. There is a proportional relationship on average between the input and output signals of the current inverters [12], so they are modelled with a gain of 250. The 6-pulse rectifier is modelled as a transfer function of the first order with a gain of 2000 and a time constant of 3.3 ms for the purposes of the simulation [29].

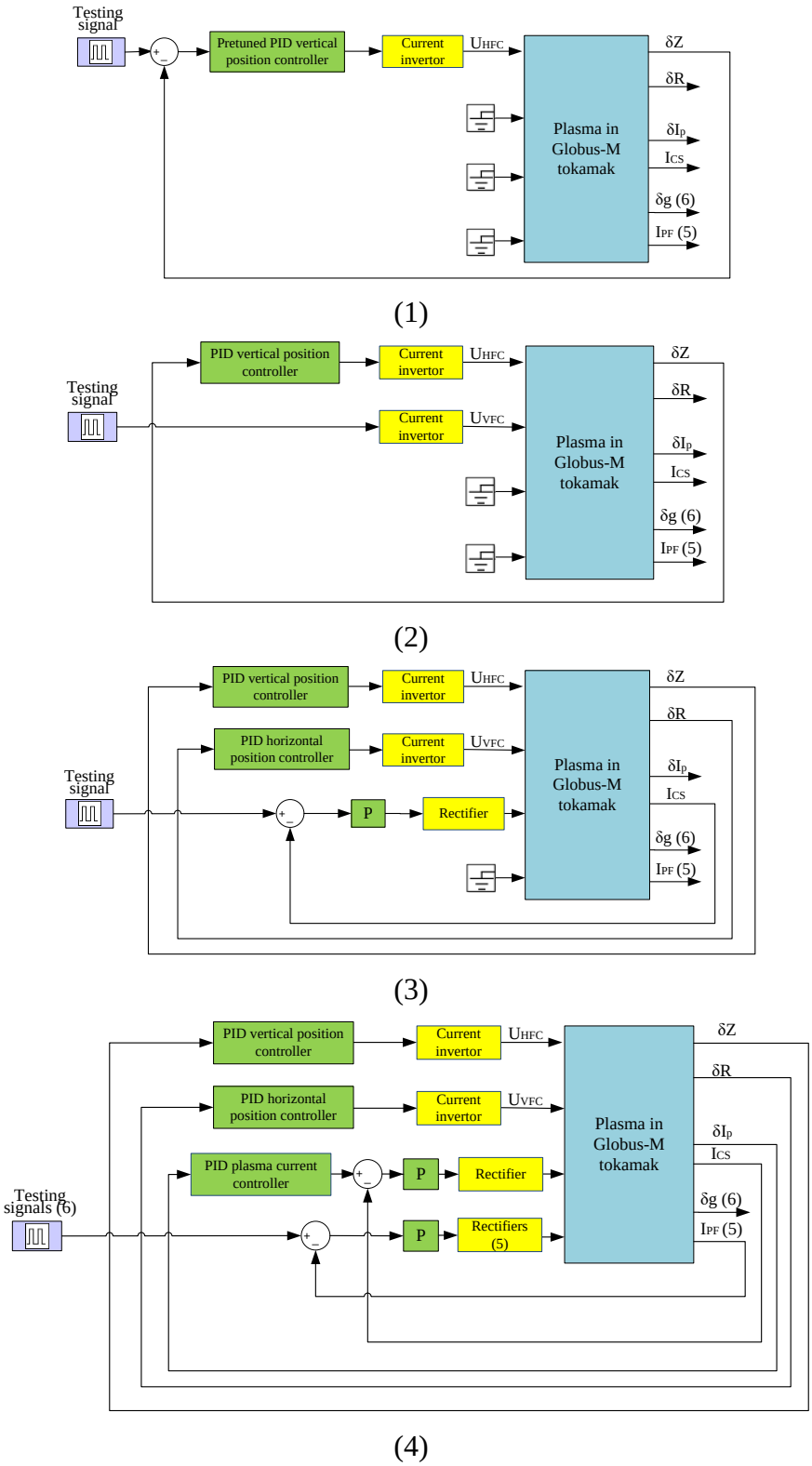

Fig. 3. Testing and identification of the system control loops: (1) vertical position control loop; (2) horizontal position control loop; (3) plasma current control loop; (4) gaps between the separatrix and the first wall control loop

The automatically tuned plasma position and current PID-controllers are presented by the transfer function as follows:

$$W_{PID}(s) = K_p + \frac{K_i}{s} + \frac{K_d s}{T_f s + 1}$$

with the following parameters:

- Vertical position PID-controller: K_p = 85, K_i = 8507.5, K_d = 0.13, T_f = 1/29981.5;
- Horizontal position PID-controller: K_p = 544.86, K_i = 25716, K_d=0, T_f = 1/2740.06;
- Plasma current PID-controller: K_p = 0, K_i = 131.79, K_d = 0, T_f = 0, P=1.

3.2. Identification of closed-loop control systems

The identification was conducted using the System Identification Toolbox from MATLAB by means of subspace methodology [13]. As a result of the loop (1) identification, the transfer function of the closed-loop system was derived. The controllers of previously tuned control loops were included in the controllable system during the identification procedure of loops (2)–(4) (Fig. 3).

The accuracy of identification of the vertical position control loop (2nd order) and the horizontal position control loop (3rd order) is 89% and 94% respectively, the plasma current control loop (9th order) is 86%, and identification of the multivariate plasma shape control loop (20th order) is ~ 80–90% for each of the loops. Figs. 4 and 5 show the transient processes for the system with the full model of the 75th order and the system with the identified models of the plasma current control loop and multivariable gaps control loop. One can see that on average the components of the transient processes coincide.

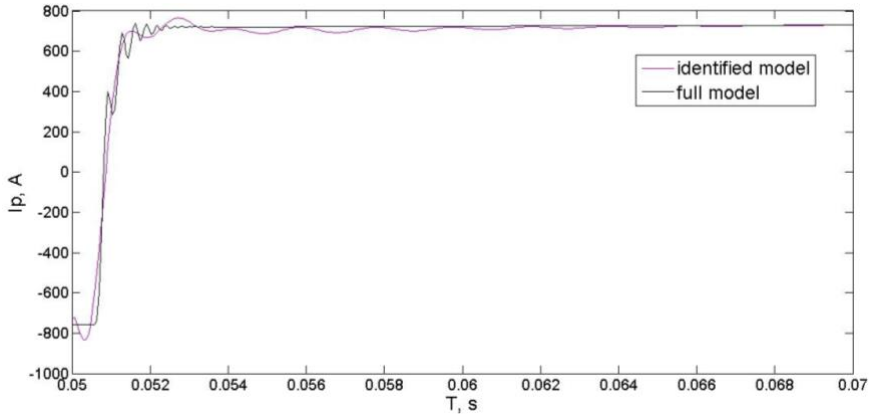

Fig. 4. Comparison of transient responses of identified and numerical experimental models for plasma current control loop

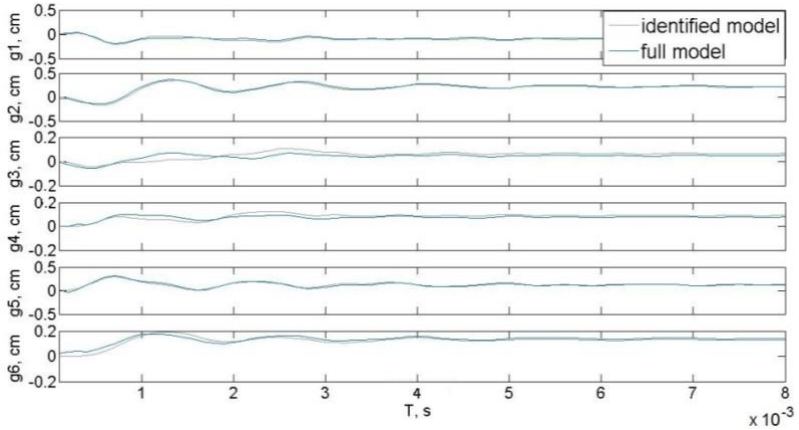

Fig. 5. Comparison of transient responses of identified and numerical experimental models for plasma shape (gaps) multivariable control loop

The results of the identification of the plasma position and plasma current loops showed that this approach makes it possible to achieve a future understanding of the application of those results to get a plasma model from the closed-loop identified transfer functions when the transfer functions of the actuator and controller are known. In this way, some results of the current inverter linear identification have been obtained in [12].

The identification procedure of the system with the plasma model to determine the gaps in the plasma shape controller design may be used directly in experiments when the plasma equilibrium reconstruction code [23, 25, 26] is connected to the tokamak outputs.

4. ROBUST H∞ LOOP SHAPING CONTROL SYSTEM DESIGN: 5 INPUTS – 6 GAPS AND SEPARATE LOOP FOR PLASMA CURRENT CONTROL

The magnetic control system for the plasma position, current, and shape in Globus-M was designed as a whole as a complex multivariable multi-loop and cascade system consisting of the following circuits (Fig. 6):

- Two loops for vertical and horizontal plasma positions control coupled via the plant (decentralised control),
- Scalar cascade circuit with the inner cascade to control the current in the central solenoid and the outer cascade to control the plasma current,
- Multivariable cascade circuit with the inner cascade to control 5 currents in the poloidal field coils and the outer cascade to control the 6 gaps.

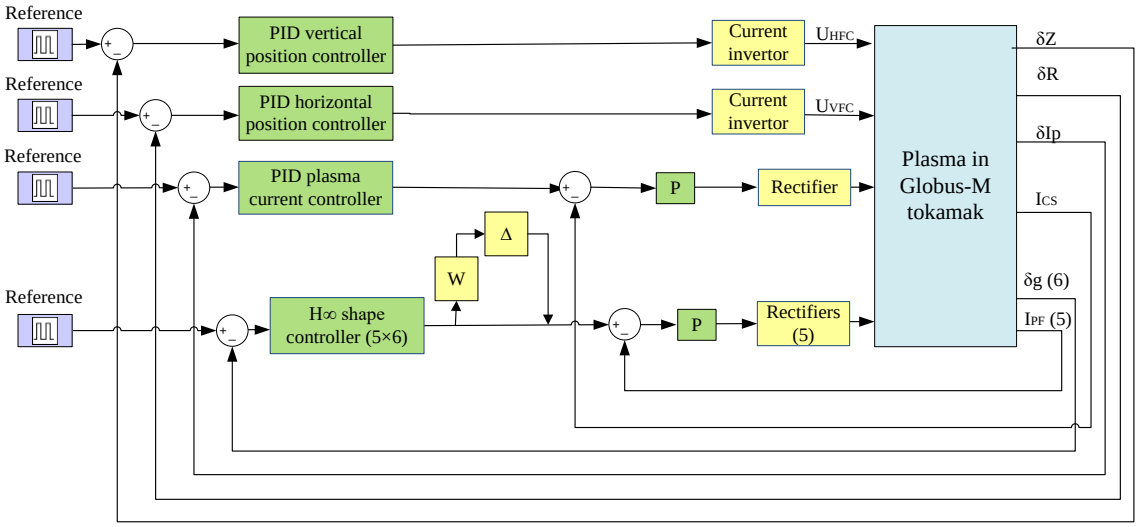

Fig. 6. Plasma position, current, and shape control system for the Globus-M tokamak

The robust loop shaping method [15, 16] was used to synthesise the multivariable controller K (which is the 5×6 size transfer matrix) for the identified transfer function of the 20^{th} order between the PF-currents references and gaps. This method is based on the normalised coprime factorisation of the transfer function of the shaped controlled model with position and currents loops containing the plasma model $G = M^{-1}N$ (see Section 2.2). The robust stability margin of the control system with the robust controller designed is $\varepsilon = 0.36$. Here $\left\|\Delta_N \ \Delta_M\right\|_\infty < \varepsilon$ is the H_∞-norm of two uncertain stable transfer functions, Δ_N and Δ_M, in the factorisation factors of the perturbed controlled model

$$G_\Delta = \left(M + \Delta_M\right)^{-1}\left(N + \Delta_N\right).$$

In doing so, the perturbed transfer function G_Δ is shaped by pre- and post-compensators

$$W_1(s) = I^{6\times 6} \times 10^6/s,\ W_2(s) = I^{5\times 5}$$

and a feedback robust controller is found to maximise ε. The final controller includes compensators and the robust H_∞-controller designed (see Section 2.2).

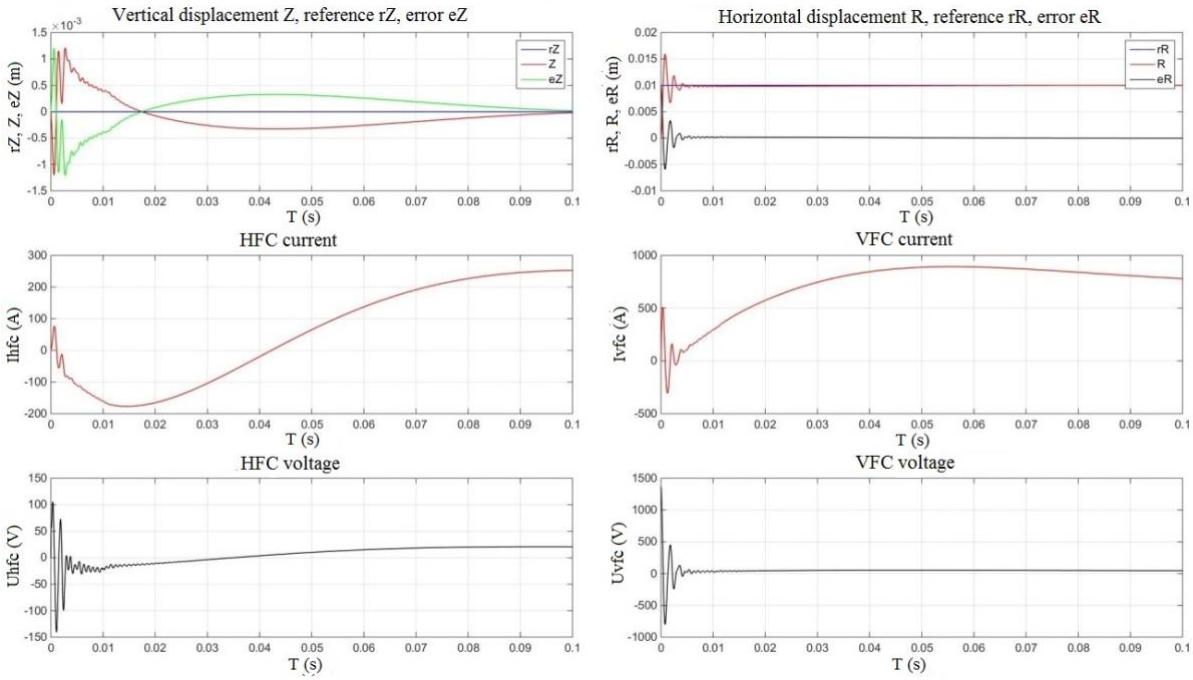

Fig. 7. Vertical and horizontal position of the plasma transient responses

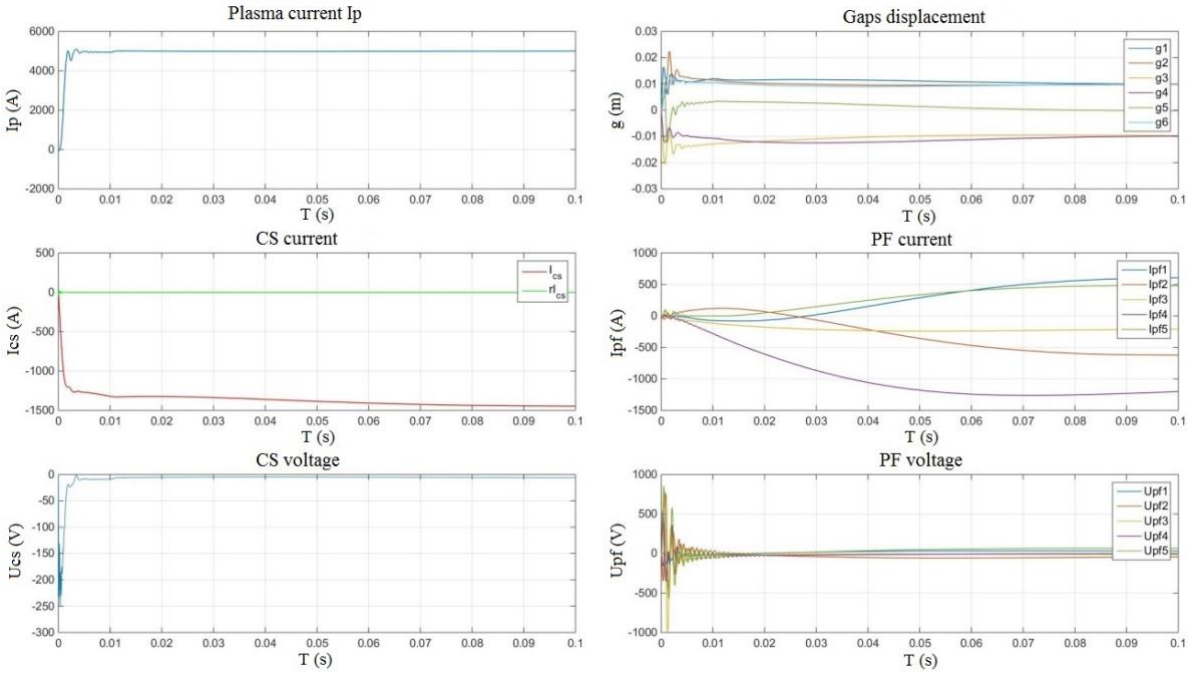

Fig. 8. Plasma current and shape transient responses

The results of the numerical simulation of the multivariable closed-loop control system are shown in Figs. 7 and 8. The following testing reference signals were fed to the input of the system to move the plasma separatrix from the initial position to the final one: 0 m to the vertical position input, 0.01 m to the horizontal position input, 5 kA to the plasma current input, and $0.01 \times [1\ 1\ -1\ -1\ 0\ 1]$ m to the plasma shape inputs (Fig. 9). The transient response time of gaps is about 0.02 s.

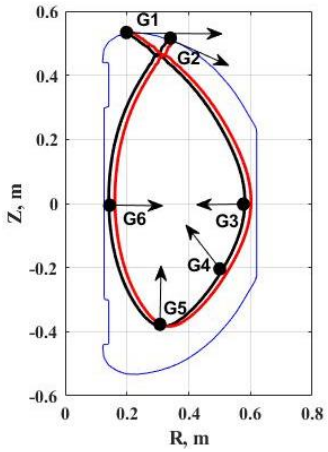

Fig. 9. Plasma separatrix displacement (the black line is the initial separatrix position, the red line is the final position) along with unit vectors for gap displacements G1-G6 and upper X-point

5. INPUT-OUTPUT ANALYSIS OF MULTI-LOOP SYSTEM STRUCTURES: 5 INPUTS – 5 GAPS, SEPARATE AND JOINT PLASMA CURRENT CONTROL

The objective of this Section is to choose the plant structure that will provide an opportunity for decentralised plasma current and shape control. The plasma position stabilisation problem has to be solved first to obtain a stable plant for plasma current and shape control system design. The plasma vertical and horizontal positions were stabilised by PID-controllers beforehand. Two alternative arrangements were considered: with joint and separate controllers for plasma current and shape. The plant for gap displacements δg (between the plasma separatrix and the first wall) control has 5 inputs ($\delta I_{ref\text{-}PF}$) and 6 outputs (δg) (Fig. 6).

A loop shaping design procedure using H_∞ synthesis was used to build the plasma shape control system (see Subsection 3.2) for the plant with 5 inputs and 6 outputs. For the purposes of engineering, it is more convenient to work with a plant that has an equal number of inputs and outputs (squared plant). Such a structure provides a possibility for decoupling of the control loops and makes it possible to use simple PID-controllers and gain matrices, which considerably simplifies the control system tuning, but still provides an opportunity to meet the basic design requirements such as speed of response, control bandwidth, robust stability, etc.

In order to design effective controllers for the squared plant model, four variants of control systems were designed: the systems with separate control for the plasma current and shape when gap 3 or 4 is eliminated, and the analogous systems with joint control (Fig. 10). For objective comparison of these four systems, 6 feedback controllers for the plasma current and shape were synthesised using the H_∞ robust loop-shaping method in line with the schemes in Fig. 10 (see Section 4), and singular value analysis [34] was carried out for these systems.

Different linear control systems for the same plant model with the same inputs and outputs may be compared in line with the same criterions in time and frequency domains. It does not matter what kind of controllers are used in that comparison in the feedback and what weighting functions have been used in the design. Designers are interested to design control systems in these conditions with maximum accuracy, speed of response, and robust stability margins. Anyway, one has to minimize the order of the linear controller in continues or discrete time. Eventually one has to choose the system which meets mostly the criteria mentioned above. This is basic aim of the designers in this research.

The frequency characteristics of the minimum singular values are constructed (Fig. 11a) for the four dynamic systems shown in Fig. 10, where the plasma current and the gaps

control loops (the latter connected by dotted lines) were opened by breaking the feedback loop at the plant model output.

One generally wants the minimum singular value $\underline{\sigma}$ of the open loop system (when breaking the loop at the *output* of the plant model at the point indicated by $\diagup$ in Fig. 10) to be as large as possible at lower frequencies where the performance of the control system is considered, and the condition number to be small [34]. A large $\underline{\sigma}$ of the open control system leads to small $\bar{\sigma}$ of the sensitivity function which links the output disturbance with the plant output.

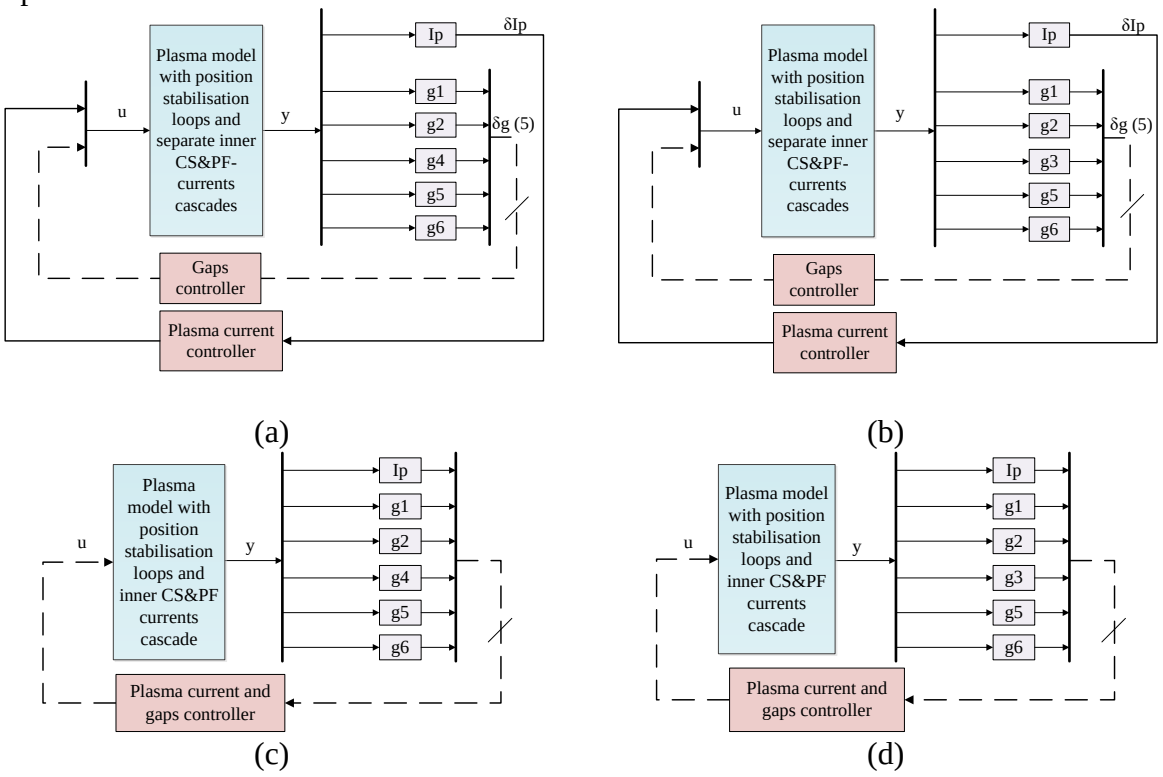

Fig. 10. Control systems: (a) separate control, gap 3 is eliminated, (b) separate control, gap 4 is eliminated, (c) joint control, gap 3 is eliminated, (d) joint control, gap 4 is eliminated

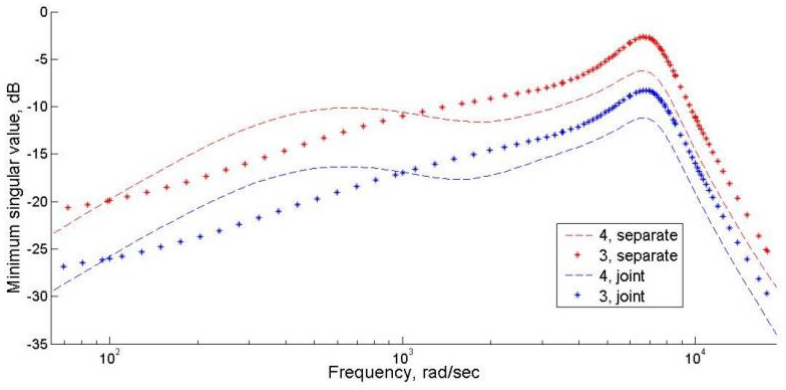

(a)

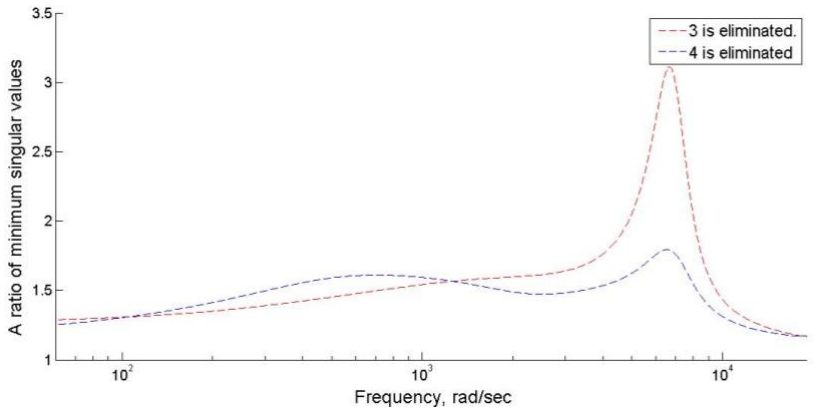

(b)

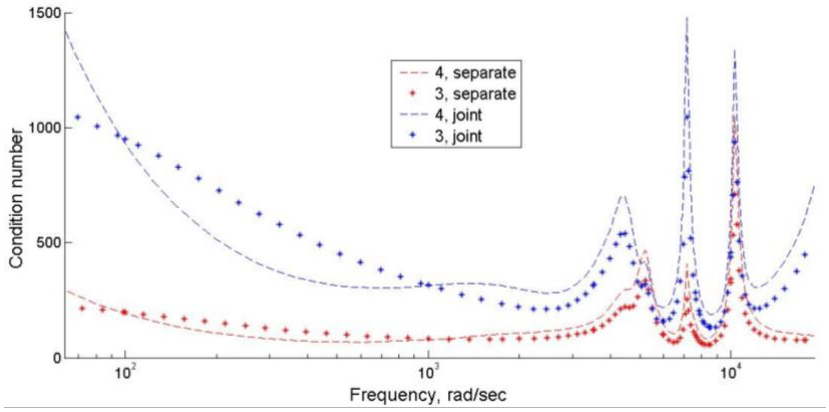

(c)

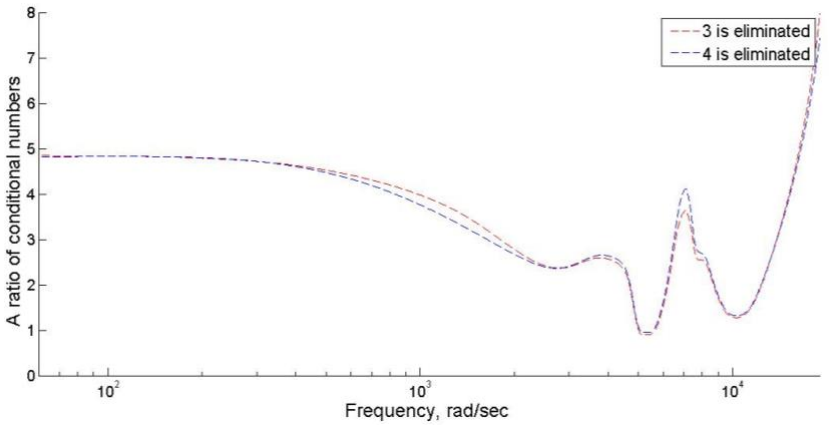

(d)

Fig. 11. (a) Minimum singular values $\underline{\sigma}$ and (c) condition numbers for 4 variants of the plant (the graph legend consists of the following components: the number of the gap which was eliminated from the system is the 3rd or 4th, the type of controller for plasma current and shape is separate or joint); (b) a ratio of the minimum singular values $\underline{\sigma}$ and (d) a ratio of the condition numbers comparing the respective values for the systems with joint and separate control (the graph legend indicates the gap that is eliminated from the system)

So

$$S(s) = \left[I + G(s)K(s)\right]^{-1}$$

is the sensitivity transfer function for the MIMO systems given in Fig. 10, where $G(s)$ is the plant model and $K(s)$ is the controller. To reduce the effects of the output disturbance on the model output, $S(s)$ should be small over the frequencies of performance interest. To reduce the sensitivity, one requires the maximum singular value of $S(s)$ to be small while

$$\underline{\sigma}(L(s)) = \underline{\sigma}\left(G(s)K(s)\right) \gg 1 \Rightarrow \bar{\sigma}\left(S\left(s\right)\right) \approx \frac{1}{\underline{\sigma}(L(s))}.$$

The frequency range for the Globus-M tokamak systems in question is 10–3000 Hz. As $\underline{\sigma}$ is larger for systems with separate control in the whole frequency range (Fig. 11 (a)), one must therefore synthesise two different controllers for current and shape.

The condition number is smaller for the system with separate control in almost the whole frequency range (Fig. 11 (c)).

Fig. 11 (b) and (d) show the quantitative difference in the minimum singular values and conditional numbers for the systems with separate and joint control. From the above, it is clear that one should choose the following structure of the system: *separate control for the plasma current and gaps and the 3rd gap should be eliminated from consideration and from the feedback of the control system*.

6. PAIRING AND H_∞ DECOUPLING PLASMA SHAPE CONTROL SYSTEM DESIGN AND SIMULATION FOR SQUARE PLANT

6.1. Pairing of the square plant: 5 inputs – 5 gaps (3rd gap is eliminated), separate plasma current control

Within the frame of the selected plant model structure, the RGA analysis [3, 34] has been applied to the multivariable transfer function $G(s)$ from the references of the inner cascade of PF-currents to the gap's displacements of the outer cascade.

There is an interaction between the controlled and manipulated variables. Inevitably, each controlled variable has an impact from all the manipulated variables through a plant. The methodology of the RGA allows one to measure the input–output interactions and choose the best pairing of variables (there are n! possible pairing configurations for the $n \times n$ plant).

There are two extreme cases that one should consider to build the RGA matrix for the system with the given plant (Fig. 12):

(a) other loops are opened $u_k = 0, k \neq j$: $\left(\frac{\partial y_i}{\partial u_j}\right)_{u_k=0,k\neq j} = g_{ij}$, $g_{ij} = \left[G\right]_{ij}$. In this case, only the selected input affects the systems outputs, which allows the effect of a certain input on each output to be measured (Fig. 12, a);

(b) other loops are closed $y_k = 0, k \neq i$: $\left(\frac{\partial y_i}{\partial u_j}\right)_{y_k=0,k\neq i} = g_{ij}$, $\hat{g}_{ij} = \frac{1}{\left[G^{-1}\right]_{ji}}$. In this case, all inputs affect all system outputs, which allows the effect of all inputs on the selected output to be measured, since the other loops are closed. In Fig. 12 (b), the signal from input u_j goes not only to the chosen output y_i but also to the other outputs and, via the feedback loops, comes to the same output y_i carrying the parasitic information of the cross-links. Here u_j is used to control y_i.

To derive the RGA matrix, one can notice that

$$y = Gu \Rightarrow \left(\frac{\partial y_i}{\partial u_j}\right)_{u_k=0,k\neq j} = \left[G\right]_{ij}, \quad u = G^{-1}y \Rightarrow \left(\frac{\partial u_j}{\partial y_i}\right)_{y_k=0,k\neq i} = \left[G^{-1}\right]_{ji}.$$

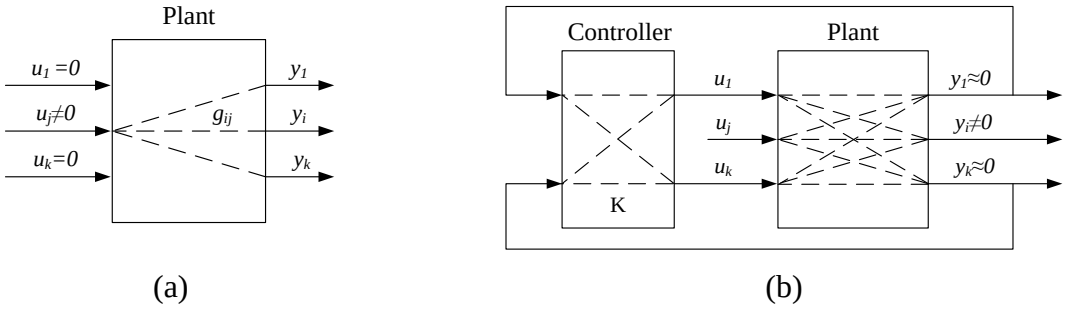

Fig. 12. Extreme RGA configurations: (a) other loops are opened, (b) other loops are closed

So the *ij*-th measure of interactions is $\lambda_{ij} = \dfrac{g_{ij}}{\hat{g}_{ij}} = \left[G\right]_{ij}\left[G^{-1}\right]_{ji}$. The RGA matrix is the corresponding matrix of relative gains (where × denotes element-by-element multiplication):

$$RGA(G(s)) = G(s) \times (G^{-1}(s))^{T}.$$

The central idea around the RGA matrix is to assess the effect that a controller of each output variable would have on a specific open loop variable. g_{ij} is the open loop gain between the *j*th input and *i*th output, $\hat{g}_{ij}$ is the resulting open loop response between the *j*th input and *i*th output when all other outputs are under control. So, the smaller the interactions between the chosen channel and the other channels, the closer the ratio of $\dfrac{g_{ij}}{\hat{g}_{ij}}$ to 1.

There are basic pairing rules that give more effective correspondence between plant outputs and inputs:

- Input–output pairing with the corresponding RGA elements closest to 1 is preferred [3];
- Large RGA elements should be avoided for input–output pairing selection [33];
- Avoid pairing on negative steady-state RGA elements. This condition is closely related to systems with lack of integrity.

$G(s)$ is the transfer function matrix of the open-loop system without a MIMO plasma shape controller, which makes it possible to rearrange the inputs and outputs of the system. The RGA matrix for the system with the 3rd gap eliminated is as follows:

$$RGA(G) = \begin{pmatrix} 7.25 & -10.83 & \mathbf{0.81} & 0.53 & 3.24 \\ \mathbf{1.73} & -13.67 & -0.88 & -1.2 & 15.03 \\ 2.03 & -6.06 & -0.11 & -0.45 & \mathbf{5.59} \\ -2.55 & \mathbf{8.37} & -0.06 & 0.78 & -5.53 \\ -7.46 & 23.19 & 1.25 & \mathbf{1.33} & -17.32 \end{pmatrix}.$$

The initial loop pairing is the following: the 1st output corresponds to the 1st input, and so on: 2-2, 3-3, 4-4, 5-5.

After RGA matrix analysis in the matrix $RGA(G)$ in line with the rules, the new input/output correspondence shown in Table 1 was obtained, which is the sequence of matrix entries highlighted in bold type.

Table 1. RGA input/output correspondence

Outputs	1	2	3	4	5
Inputs	3	1	5	2	4

In accordance with Table 1, one can construct a matrix H of the discovered input/output correspondence that may be connected to plant inputs for further controller design:

$$H = \begin{bmatrix} 0 & 0 & 1 & 0 & 0 \\ 1 & 0 & 0 & 0 & 0 \\ 0 & 0 & 0 & 0 & 1 \\ 0 & 1 & 0 & 0 & 0 \\ 0 & 0 & 0 & 1 & 0 \end{bmatrix}.$$

6.2. Design of plasma shape control system with additional channel decoupling by H_∞ fixed structure tuning

When the control system structure was analysed and the most effective loop pairing was found, the control problem arose. The structured H_∞ synthesis helps one to build a decoupling controller [4, 6]. All control elements were tuned using the *looptune* command in MATLAB [4]. This command automatically converts the target bandwidth, performance requirements, and additional design requirements into weighting functions that express the requirements as an H_∞ optimisation problem. The optimisation of the H_∞ mixed-sensitivity norm S (S is the sensitivity) allows one to tune the controller:

$$\left\| \begin{matrix} W_1 S(K) \\ W_2 \left(I - S(K) \right) \end{matrix} \right\|_\infty \xrightarrow{K} \min,$$

where W_1, W_2 are weighting functions. Automatic tuning of all feedback loops (PI-controllers and decoupling matrix D) for the system with the eliminated 3rd gap and appropriate loop pairing has been done (Fig. 13).

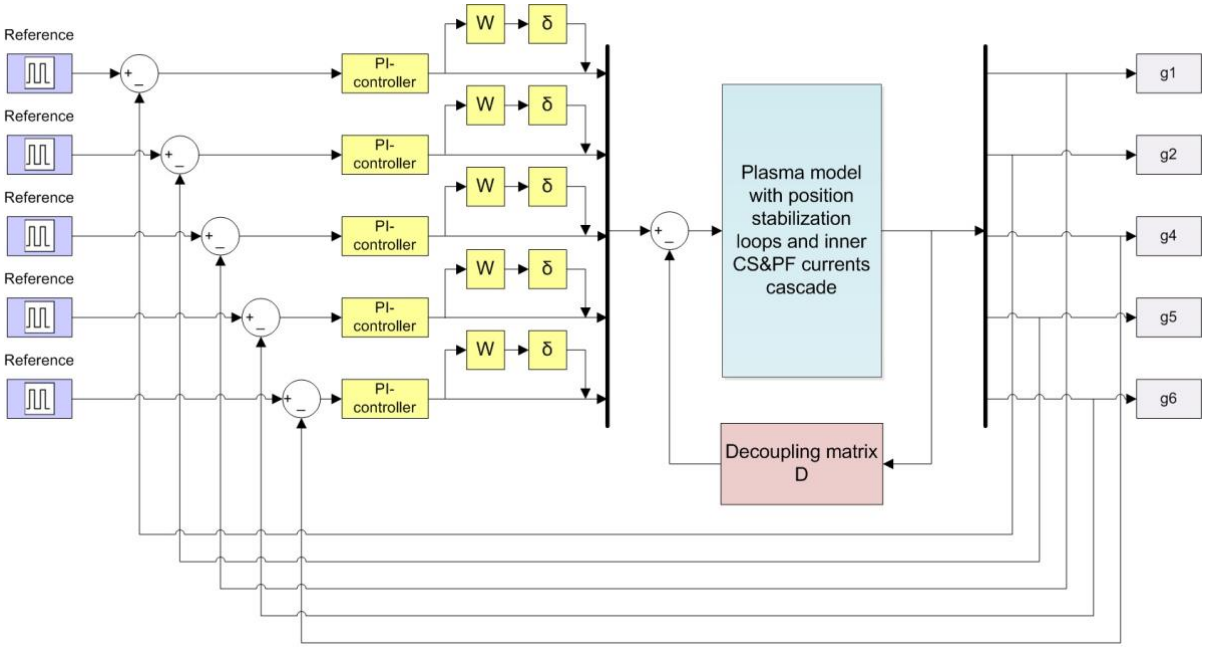

Fig. 13. Structural scheme of output-input pairing, multivariable PI-controller and D-decoupling matrix for Globus-M

When the control system is tuned, the decoupling matrix `D` ensures that each output of the controlled `PLANT` tracks the corresponding reference signal with minimal crosstalk. To tune the control system, including the decoupling matrix `D`, one first creates a numeric model of the plant. Then one creates tunable models of the controller elements and interconnect them to build a controller model. Then one uses *looptune* command to tune the free parameters of the controller model. Finally, one has to examine the performance of the tuned system to confirm that the tuned controller yields desirable performance.

7. COMPARISON OF THE TWO SYSTEMS

7.1. Performance analysis by means of simulations

The systems with two types of controllers, namely, the H_∞ controller synthesised by the robust loop shaping method (H_∞ loop shaping controller) and the controller synthesised and automatically tuned on the basis of structural analysis, the RGA matrix, and structured H_∞ synthesis (double *RGA*-H_∞ decoupling controller), have been compared.

The responses of the systems to the following reference

$$g_{\text{ref}} = g\times[1\ 1\ -1\ -1\ 0\ 1],\ g = \begin{cases} 4t,\ 0 < t < 0.005, \\ 0.02,\ t \geq 0.005, \end{cases}$$

are shown in Fig. 14. The minus sign corresponds to the plasma moving to the first wall. The gap tracking errors are presented in Fig. 15. The response time is approximately 10 ms and the maximum deviation of gaps is about 0.75 cm for the former system and 0.5 cm for the latter system. The steady-state errors are 0.24 cm for the former system and 0.13 cm for the latter system (Fig. 15, Table 2).

Table 2. Comparison of the maximum deviation $D_{\max}$ of gaps and the steady-state errors E_{ss}

Gaps	H_∞ loop shaping controller		*RGA*-H_∞ decoupling controller	
	$D_{\max}$, m	E_{ss}, m	$D_{\max}$, m	E_{ss}, m
g1	0.0031	0.0013	0.0071	0.0001
g2	0.0034	0.0019	0.0045	0
g3	0.005	0.0006	–	–
g4	0.0027	0.0018	0.002	0
g5	0.007	0.0006	0.002	0
g6	0.0025	0.0025	0.0016	0.0011

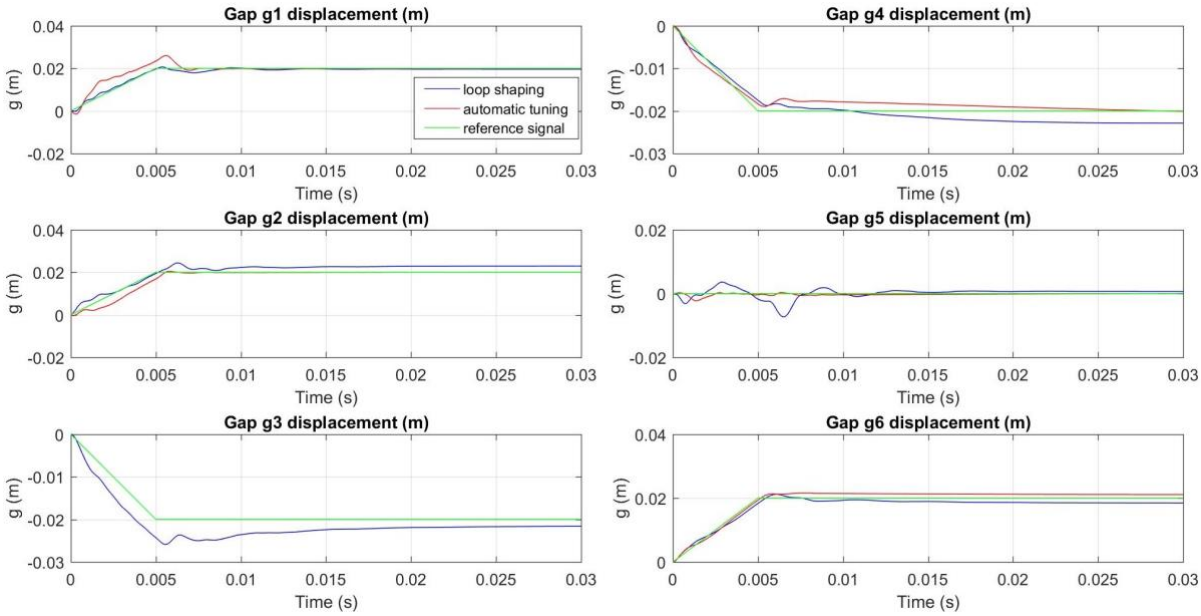

Fig. 14. Reference response of the plasma shape control systems in Globus-M

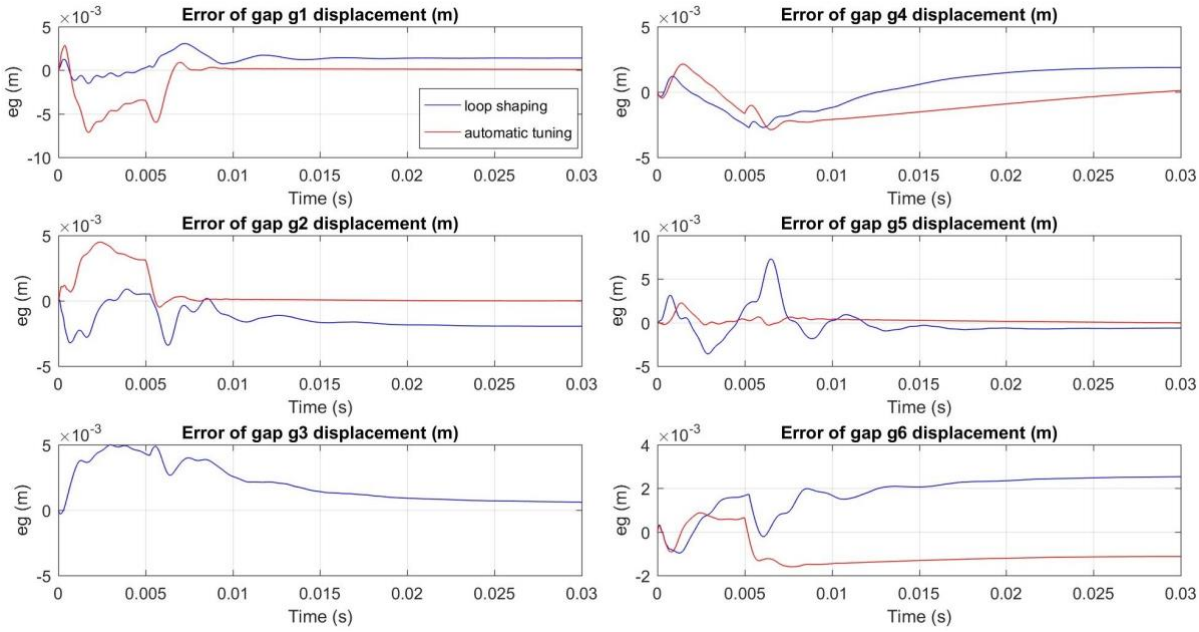

Fig. 15. Gap tracking errors

Tuning the PI-controllers' parameters and decoupling matrix D by means of the *looptune* command for the latter system from an unstable initial guess took 25 iterations and about 3 minutes in the MATLAB environment.

Figs. 9 and 14 show how the plasma separatrix moved during the simulation. The separatrix is the plasma boundary in the poloidal plane and may be found as the largest closed level line of the poloidal flux [1].

7.2. Robust stability analysis

7.2.1. Singular value analysis

A plant model additive disturbance Δ was added into the systems to evaluate the robust stability margins that the two control systems could provide [36]. The structural schemes of the plasma shape control systems in Globus-M with additive disturbance are shown in Fig. 16. The transfer functions for the known parts of the systems connecting the uncertainty output and input v→u are as follows:

(a) $H = -K\left(I + GK\right)^{-1}$,

(b) $H = -\left(I + \left(K + D\right)G\right)^{-1}\left(K + D\right)$.

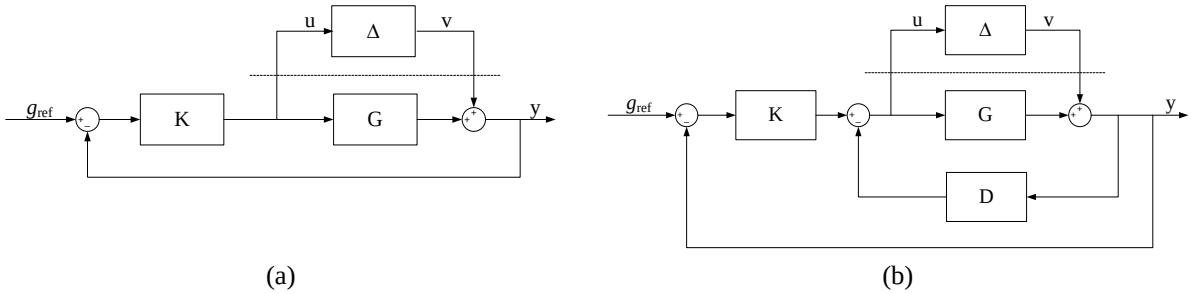

(a) (b)

Fig. 16. Structural schemes of the plasma shape control systems in Globus-M with additive plant model disturbance: (a) system with H_∞ controller synthesized by loop shaping method, (b) system with controller synthesized on the basis of structural adjustment

From the small gain theorem [36], it is deduced that the robust stability margin of the system can be obtained as follows:

$$\|\Delta\|_\infty < \frac{1}{\|H\|_\infty}.$$

The maximum singular values and the corresponding values of the robust stability margins for the given systems are represented in Fig. 17 and Table 3.

However, the H_∞ robust loop-shaping controller provides a considerably greater robust stability margin at additive plant uncertainty. Compared to the system with the controller synthesised on the basis of structural adjustment, it allows the system with the H_∞ controller synthesised by the loop shaping method to ensure a roughly two and a half times higher robust stability margin (Table 3).

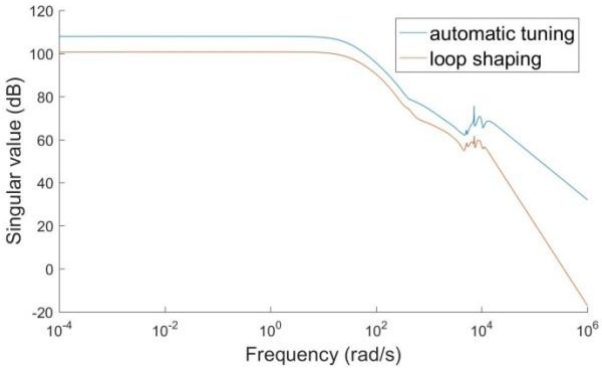

Fig. 17. Maximum singular values

Table 3. Robust stability margins

Method / Type of the system	Singular value analysis	μ-analysis
(a) H_∞ loop shaping controller	8.91×10^{-6}	1.17
(b) H_∞ decoupling controller	3.98×10^{-6}	1.34
The ratio of robust stability margins of system (a) to (b)	2.23	0.87

7.2.2. μ-analysis

A lot of dynamic perturbations may occur in different parts of the system. In particular, in our research, we used a multiplicative input uncertainty. However, they can all be pulled out into one perturbation block Δ, represented by the block-diagonal matrix

$$\Delta = \left\{ diag\left[\delta_1 I_{r_1} \ldots \delta_s I_{r_s} \right] :\ \delta_i \in C \right\},$$

where $\sum_{i=1}^{s} r_i = n$ and n is the dimension of the block Δ. This representation (Figs. 6 and 13) of the systems made it possible to test the robust stability of the closed-loop system (W is a weighting function).

The frequency response plots of the structured singular values μ [30]

$$\mu^{-1}(M) := \min_{\Delta\in\Delta} \left\{ \bar{\sigma}(\Delta) : \det(I - M\Delta) = 0 \right\}$$

were examined to determine the system with the highest robust stability margin (Fig. 18).

From the small gain theorem, one may deduce that the smaller the μ, the higher the robust stability margin. The μ analysis was conducted for $M\Delta$ configurations of the systems. For the system with the H_∞ controller synthesised by the loop shaping method, the μ peak equals 1.17 and is less than for the system with controller synthesised on the basis of structural analysis, which is equal to 1.34 (Table 3). As the structured singular value μ is the direct measure of the robust stability margin of the closed loop system with uncertainties, it was therefore clear that the former system has the higher robust stability margin.

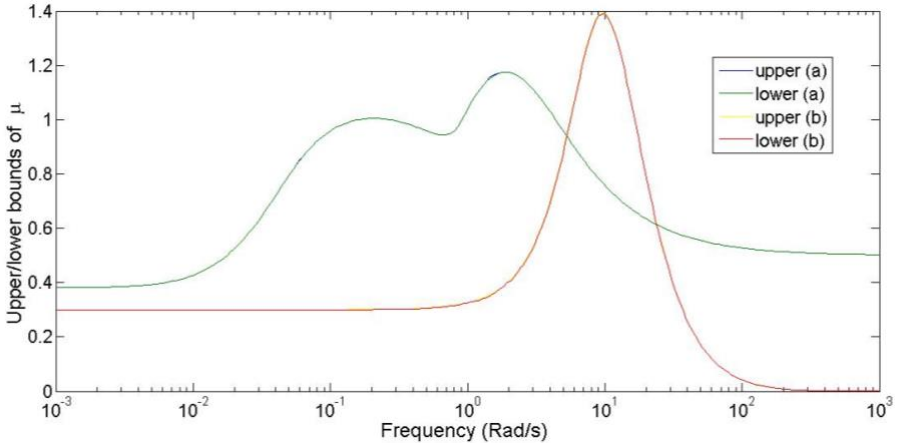

Fig. 18. Structured singular values μ for: (a) system with H_∞ controller synthesised by loop shaping method; (b) system with controller synthesised on the basis of structural adjustment

The interpretation of the robust stability analysis results obtained by the structured singular value μ- and singular values showed that the conclusions are consistent.

8. CONCLUSION

To summarise, the double decoupling approach is proposed for the plasma shape control system design. This novel cascade RGA-H_∞ double decoupling magnetic control system was compared with the H_∞ loop shaping design control system in terms of robustness and performance. The first one deals with structural decisions that must be made before starting the controller design. The system reduction using identification which, in turn, makes it possible to reduce an order of controller, provides the basis for the second one.

These two approaches were applied for plasma shape control in the Globus-M tokamak. The H_∞ loop shaping controller, which uses a combination of loop shaping and robust stabilisation, was designed for the reduced plasma model. Identification subspace methodology was applied to linear plasma models to reduce their high order to an essential lower order to design plasma current and shape multivariable control systems. The H_∞ double decoupling fixed-structure controller was designed for the plasma shape control linear model, which consists of two feedback loops: the inner loop provides decoupling and the outer loop also provides decoupling and the desired setpoint tracking performance. The first approach results in good robustness (the ratio of the robust stability margins of the latter system to the former system is more than one), whereas the second one made it possible to find the control system structure that ensures better time-domain performance (the maximum deviation of gaps and the steady-state errors are about 50% less for the second control system).

In future, it is intended to introduce the control systems designed into experiments on the Globus-M2 tokamak [8] on the base of the real time testbed being developed in [19].

ACKNOWLEDGEMENTS

The authors thank research associate P.S. Korenev (V.A. Trapeznikov Institute of Control Sciences of the Russian Academy of Sciences, Moscow, Russia) for the plasma linear models designed on the basis of the experimental data of the Globus-M tokamak.
This work was supported by the Russian Science Foundation (RSF) under Grant numbers 17-19-01022 and 21-79-20180.

REFERENCES

1. Ariola, M. and Pironti, A. (2016). *Magnetic control of tokamak Plasmas*. Springer, 2nd ed.

2. Bakharev, N.N., Bulanin, V.V., Chernyshev, F.V., et al. (2018). The effect of increasing toroidal magnetic field in the Globus-M spherical tokamak. *Nuclear Fusion*, 58(12), 126029. DOI: https://doi.org/10.1088/1741-4326/aae60d

3. Bristol, E.H. (1966). On a new measure of interactions for multivariable process control. *IEEE Trans. Aut. Control*, AC-11, 133–134.

4. Gahinet, P. and Apkarian, P. (2011). Decentralized and fixed-structure H_∞ control in MATLAB. *Proc. 50th IEEE Conference on Decision and Control and European Control Conference (CDC-EDC)*, 8205–8210.

5. Gossner, J.R., Vyas, P., Kouvaritakis, B., and Morris, A.W. (1999). Application of cautious stable predictive control to vertical positioning in COMPASS-D tokamak. *IEEE Trans. Control Syst. Technol.*, 7(5), 580–587. DOI: 10.1109/87.784421

6. Gu, D.-W., Petkov, P.Hr. and Konstantinov, M.M. (2005). *Robust control design with Matlab*. Springer.

7. Gusev, V.K., Azizov, E.A., Alekseev, A.B., et al. (2013). Globus-M results as the basis for a compact spherical tokamak with enhanced parameters Globus-M2. *Nuclear Fusion*, 53(9), 093013. DOI: https://doi.org/10.1088/0029-5515/53/9/093013

8. Gusev, V.K, Bakharev, N.N., Belyakov, V.A., et al. (2015). Review of Globus-M spherical tokamak results. Nuclear Fusion, 55(10), 104016. DOI: https://doi.org/10.1088/0029-5515/55/10/104016

9. Gusev, V.K., Bakharev, N.N., Ber, B.Ya., et al. (2016). Globus-M plasma physics research for fusion application and compact neutron source development. *Plasma Physics and Controlled Fusion*, 58(1), 014032. DOI: https://doi.org/10.1088/0741-3335/58/1/014032

10. Kadurin, A.V. and Mitrishkin, Y.V. (2011). Multidimensional system of cascaded control of plasma form and current in tokamak with channel decoupling and H_∞-controller. *Automation and Remote Control*, 72(10), 2053–2070. DOI: https://doi.org/10.1134/S0005117911100067

11. Korenev, P.S., Mitrishkin, Y.V., Patrov, M.I. (2016). Rekonstrukciya ravnovesnogo raspredeleniya parametrov plazmy tokamaka po vneshnim magnitnym izmereniyam i postroenie lineinykh plazmennykh modelei [Reconstruction of equilibrium distribution of tokamak plasma parameters by external magnetic measurements and construction of linear plasma models]. *Mechatronics, Automation, Control*, 17(4), 254–265, [in Russian].

12. Kuznetsov, E.A., Mitrishkin, Y.V., Kartsev, N.M. (2019). Current inverter as self-oscillating actuator in applications for plasma position control systems in the Globus-M/M2 and T-11M tokamaks. *Fusion Engineering and Design*, 143, 247–258. DOI: https://doi.org/10.1016/j.fusengdes.2019.02.105

13. Ljung, L. (1999). *System identification: theory for the user*. Prentice Hall.

14. Ljung, L. (2015). *System identification toolbox: user's guide, R2015b*. The MathWorks, Inc.

15. McFarlane, D.C. and Glover, K. (1992). A loop shaping design procedure using H_∞ synthesis. *IEEE Trans. Aut. Control*, 37(6), 759–769. DOI: 10.1109/9.256330

16. McFarlane, D.C. and Glover, K. (1989). *Robust controller design using normalized coprime factor plant descriptions (Lecture notes in control and information sciences)*. Springer Verlag.

17. Minaev, V.B., Gusev, V.K., Sakharov, N.V., et al. (2018). First results of plasma experiment on the spherical tokamak Globus-M2. *Proc. 45th EPS Conference on Plasma Physics*, ECA 42A P4-1065.

18. Minaev, V.B., Gusev, V.K., Sakharov, N.V., et al. (2017). Spherical tokamak Globus-M2: design, integration, construction. *Nuclear Fusion*, 57(6), 066047. DOI: https://doi.org/10.1088/1741-4326/aa69e0

19. Mitrishkin, Y.V. Plasma magnetic control systems in D-shaped tokamaks and imitation digital computer platform in real time for controlling plasma current and shape. *Advances in Systems Science and Applications* [in print].

20. Mitrishkin, Y.V., Golubtsov, M.P. (2018). A hybrid control system for an unstable non-stationary plant with a predictive model. *Automation and Remote Control*, 79(11), 2005–2017. DOI: https://doi.org/10.1134/S000511791811005X

21. Mitrishkin, Y.V., Kartsev, N.M., Pavlova, E.A., Prokhorov, A.A., et al. (2018). Plasma control in tokamaks. Part 2. Magnetic plasma control systems. *Advances in Systems Science and Applications*, 18(3), 39–78. DOI: https://doi.org/10.25728/assa.2018.18.

22. Mitrishkin, Y.V., Korenev, P.S., Kartsev, N.M., Kuznetsov, E.A., Prokhorov, A.A., and Patrov, M.V. (2019). Plasma magnetic cascade multiloop control system design methodology in a tokamak. *Control Engineering Practice*, 87, 97–110. DOI: https://doi.org/10.1016/j.conengprac.2019.03.018

23. Mitrishkin, Y.V., Korenev, P.S., Kartsev, N.M., Patrov, M.I. (2014). Plasma shape control with a linear model for Globus-M tokamak. *Proc. 41st EPS Conference on Plasma Physics*, P4.054.

24. Mitrishkin Y.V., Korenev P.S., Prokhorov A.A., Kartsev N.M., Patrov M.I. (2018). Plasma Control in Tokamaks. Part 1. Controlled thermonuclear fusion problem. Tokamaks. Components of control systems. *Advances in Systems Science and Applications*, 18(2), 26-52. DOI: https://doi.org/10.25728/assa.2018.18.2.598

25. Mitrishkin Y.V., Prohorov A.A., Korenev P.S., Patrov M.I. (2017). The method of formation of the model of magnetic control of plasma shape and current with feedback. Patent of the Russian Federation for invention No. 2702137. Priority of invention: April 28, 2017. Date of registration: October 4, 2019.

26. Mitrishkin, Y.V., Korenev, P.S., Prohorov, A.A., Patrov, M.I. (2017). Tokamak plasma magnetic control system simulation with reconstruction code in feedback based on experimental data. Proc. IEEE 56th Annual Conference on Decision and Control, Melbourne, Australia, December 2017, 2360–2365.

27. Mitrishkin, Y.V., Korostelev, A.Y., Dokuka, V.N., Khayrutdinov, R.R. (2011). Synthesis and simulation of a two-level magnetic control system for tokamak-reactor plasma. *Plasma Physics Reports*, 37(4), 279–320. DOI: https://doi.org/10.1134/S1063780X1103010X

28. Mitrishkin, Y.V., Kurachi, K., Kimura, H. (2003). Plasma multivariable robust control system design and simulation for a thermonuclear tokamak-reactor. *International Journal of Control*, 76(13), 1358–1374. DOI: https://doi.org/10.1080/0020717031000149951

29. Mitrishkin, Y.V., Pavlova, E.A., Kuznetsov, E.A., Gaydamaka, K.I. (2016). Continuous, saturation, and discontinuous tokamak plasma vertical position control systems.

Fusion Engineering and Design, 108, 35–47. DOI: https://doi.org/10.1016/j.fusengdes.2016.04.026

30. Packard, A. and Doyle, J. (1993). The complex structured singular value. *Automatica*, 29(1), 71-109. DOI: https://doi.org/10.1016/0005-1098(93)90175-S

31. Pavlova, E.A. and Mitrishkin, Y.V. (2015). Identifikaciya i mnogokonturnoe upravlenie polozheniem tokom i formoj plazmy v tokamake Globus-M [Identification and multi-loop control systems for plasma position, current, and shape in Globus-M tokamak]. *Proc. 7th All-Russian scientific-practical conference "Simulation. Theory and Practice" (IMMOD)*, 270–274, [in Russian].

32. Pavlova, E.A., Mitrishkin, Y.V., Khlebnikov, M.V. (2017). Control System Design for Plasma Unstable Vertical Position in a Tokamak by Linear Matrix Inequalities. *Proc. 11th IEEE International Conference on Application of Information and Communication Technologies (AICT)*, 458–462.

33. Skogestad, S. and Morari, M. (1987). Implications of large RGA elements on control performance. *Industrial & Engineering Chemistry Research*, 26, 2323–2330. DOI: https://doi.org/10.1021/ie00071a025

34. Skogestad, S. and Postlethwaite, I. (2005). *Multivariable feedback control*. *Analysis and design*. John Wiley and Sons, Ltd, 2nd ed.

35. Yuan, Q.P. et al. (2013). Plasma current, position and shape feedback control on EAST. *Nuclear Fusion*, 53, 043009. DOI: https://doi.org/10.1088/0029-5515/53/4/043009

36. Zhou, K. and Doyle, J.C. (1998). *Essentials of robust control*. Prentice Hall.

